Available Online at www.ijcsmc.com

International Journal of Computer Science and Mobile Computing

A Monthly Journal of Computer Science and Information Technology

ISSN 2320–088X
IMPACT FACTOR: 7.056

IJCSMC, Vol. 14, Issue. 11, November 2025, pg.85 – 101

High-Performance Steganography Using an Ensemble InceptionV2-Wavelet Model with ABC Algorithm Optimization

V. ARUNKUMAR[1]; Dr. K. PADMANABHAN[2]

[1]Ph.D Research Scholar, Department of Computer Science, Periyar University, Salem, India
[2]Controller of Examinations, Vivekanandha College of Arts and Sciences for Women (Autonomous), Tiruchengode, India
[1] veere.arun@gmail.com; [2] padmaindia75@gmail.com

DOI: https://doi.org/10.47760/ijcsmc.2025.v14i11.006

Abstract: Image Steganography refers to the practice of concealing information within an image. Therefore, we can utilize this to send any confidential data in a secure way. But traditional image steganography methods have poor security and can be easily attacked by steganalysis to reveal the secret data hiding behind images. As the new image steganography technique, this project introduces the use of both Inception V2 and wavelet transform. Ascension 2 Convolutional neural networks, or Inception V2, have several uses in the field of image processing.Abstract Image decomposition using wavelet transform is one of the keys tools in hiding secret data within images, which provides a vigorous way of in hiding the secret information within the outcomes of the transformation that are not effortlessly evident. The proposed Inception V2 based autoencoder model has an accuracy on the first dataset Dataset 1 at 91.00% on comparison with three data sets.

Keywords: Inception V2, Wavelet Transform, Autoencoder Model, Secret Data Concealment, Steganalysis.

I. INTRODUCTION

Images gathering (image) and data hiding in them among the two key parts of image stenography [1]. Since transmission of data is largely data and privacy protection, this makes and image steganography become an important issue [2]. Now more than ever, the demand for higher standards of security and privacy is at an all-time high [3]. This is due to the ever emerging new technologies and the levels of dependability on the data communications as well as the type of the information it holds. No matter how many protocols and apps try to keep bad guys from getting past security measures, they will always be able to out-plan them. The risk of intercepting sensitive information and conversations is increasing due to the daily emergence of new threats [4]. Therefore, the new study's authors think it's crucial to keep investigating the many security threats connected with data transmission. The practice of picture steganography, a branch of information security, is centred on the idea of using concealed images to hide information.Steganography is predominately focused on the utilization of images [5], despite the fact that there are other methods of information security that also play important roles. Cryptographic technologies have long been regarded as the most efficient means there are to conceal information. On the other hand, not all of the information is concealed. Instead of reading the content, they will rather convert it to an unintelligible format [6]. The secret format of encryption techniques may be seen, and there are powerful computers and programmes that can decipher even the most complex algorithms [7]. Consequently, encryption methods are not foolproof. This makes it possible for hackers to decipher information that has been encrypted. There is a necessity for this, as a direct result of the ever-changing nature of the threats that we face in order to protect one's data in a way that is not only reliable but also efficient. Finding steganographic algorithms that can provide security while simultaneously protecting data secrecy is of the utmost importance. A steganography tool is offered as part of this research so that safety can be better ensured that is present during the process of data transfer. A plethora of steganographic techniques for protecting data transmission have emerged in recent years [8–11]. Using methods analogous to encryption, steganography is the art of data concealment. The majority of the time, steganographic techniques that are appropriate for the world of many media wind up garnering a significant amount of popularity [8]. When seen from a different angle, the technique of invertible image steganography has also shown substantial utility [9]. Steganography in the JPEG file format using content that is identical has also shown to have great utility [10]. Another method that tries to increase payload capacity and has received a lot of attention is the method of hybrid algorithms for space-bound image steganography at a low level [11]. This method employs a pair of distinct algorithms. In contrast, the Least Significant Bit (LSB) approach is dynamic and subject to constant refinement [12-14].

II. LITERATURE REVIEW

To ensure success, it is essential to stick to the previous research while you verify that the selected steganographic method is strong and very reliable. Using a Multi-Layer Security Strategic approach, this study aims to give a solution for increasing stenographic security. This strategy entails employing a variety of event-driven security routines, and their application is the study's primary objective. This tool will strengthen the protection afforded to the confidential text message on a wide variety of different protection levels. This research considers how to use a picture's least significant bit (LSB). The use of cryptographic methods can bolster steganography, which is another form of covert communication [15]. Steganography can also be usedto hide information. The techniques of spatial picture steganography have been the subject of a significant number of previous investigations. Recently, the LSB technique has seen a significant uptick in popularity. The LSB replacement is a suitable and straightforward procedure that may be used to insert data into a cover picture [13].

A more effective method for concealing data in very noisy areas of a picture was suggested in [16]. This strategy depends on the spatial approach that is taken. The secret is in using deep neural networks to the success of this article's primary focus, which is the capacity to conceal information up to eight times more successfully than is possible with ordinary LSB. Nevertheless, the picture serving as the cover for the hidden message must adhere to certain criteria established from what the network test yielded. Consequently, this method cannot be applied to any image. There is an increase in the approach's complexity and execution costs due to the use of networks. The results of training and testing the neural network that was detailed in were very accurate [16] on random photos using the ImageNet database. A spatial technique is used in the enhanced method that was proposed in [17] for concealing information within an image. The authors mapped characteristics or components to identify the best and safest locations to conceal the picture, using a real image and faster algorithms for region-based convolutional neural networks. To do this, they first needed to determine where the picture would be most discreetly hidden. In addition to LSB, the extremely undetectable stego algorithm was utilized, which gave an even higher level of privacy while also increasing the sum of all bits.

This paper's writers [18] proposed a method to encrypt sensitive data by first compressing it, before establishing an encryption using the Advanced Encryption Standard technique mechanism for the encoded and compressed data. Finally, in order to ensure that their existence would not affect the main text, they were inserted into the Arabic language using certain letters and places. Another option put out was the implementation of protocols that are implicit inside the material, such as in the layout, lyrics, or images. By adopting an LSB approach, the authors of [19] were able to conceal personal information prior to it being communicated. In [20], the authors investigated when deep learning may be useful for steganography to protect inference privacy. In particular, they wanted to know when deep learning would be the best choice. A considerable number of concerns pertaining to steganography have been illuminated by previous investigations that were carried out in the past and have provided new insights. As far as is practically possible, using involved matrices and functional steganography, It is necessary to enhance the quantity of individuals engaging in counting-based secret sharing [21]. Reason being, secret sharing depending on participant counts is really necessary. This is of the utmost importance since it is possible to produce secure communication by basing it on a rapid response, which is connected with robust concealing [22]. This is why it is so important. Furthermore, a spatial image steganography using a GAN and a cross-feedback mechanism was created by the authors of the aforementioned research [23]. One typical method for preventing the revealing of personally identifiable information is to enhance grayscale steganography [24]. To ensure the confidentiality of the information, this is done. Because of this, the authors of [25] devised a system of chaotic video steganography to conceal various covert messages in various settings.The authors did this in order to use this technique across a variety of situations. In [26], moreover, the researchers explored the robust of break-proof, XOR operation-based evolutionary algorithm for untraceable image steganography in discrete wavelet transform. A special type of image disentanglement autoencoder used in steganography above has the highest security level [27] when it comes to steganography without data embedding. In [28], Based on combining steganography, the authors devised a four-step process for data security with cryptography that was aimed at protecting data stored in the cloud against unauthorized access. Such a model was designed for protecting cloud-computing data. In recent years, a means of secretly embedding data into protected images using the evolutionary algorithm and the ballot transform were proposed in [29]. DNA nano sensing devices have been recently shown to detect metal ions and molecular crypto-steganography for configurable sensitivity [30]. This was relatively recently discovered.

III. METHODOLOGY

DATASET:

We will be using the UCI dataset for this project. You have X-Rays, MRI Scans, CT Scans, etc. in different categories of medical DICOM images from various sources, it is an intermediate to advanced level dataset with images. It is a diverse dataset and can get the performance of the Inception V2 model.
Link: -"https://www.kaggle.com/datasets/kmader/siim-medical-images?select=tiff_images"

PREPROCESSING:

PreprocessingLordGranville - The following Three preprocessing steps are applied to each of our sentences, as follows:

IMAGE NORMALIZATION:

Involves normalizing the pixel values in the image to a range 0 and 1. It helps to increase the performance on the Inception V2 model.

IMAGE DENOISING:

Which is nothing but removing the noise from the image. This way, it will make the image look better and the Inception V2 model will work better.

WAVELET TRANSFORM:

The image degrades due to a low resolution of images and wavelet coefficients used to describe them. Subsequently, these coefficients can be utilized to embed code in a picture where the code is simply about impossible to be identified.

OPTIMIZER:

Further, we will be using ABC optimizer for hyperparameter tuning. It yields optimal hyperparameters far faster than its traditional counterparts, being a meta-heuristic algorithm;

EVALUATION AND COMPARISON: TESTING

1. Steganographic algorithm performance will be assessed according to the following metrics:
2. DWT coeicents are useful for determining the maximum amount of hidden data that an image can contain.The peak-to-noise ratio (PSNR) is one way to measure the quality of a stego image.
3. To find out how close the two images are to one another, one might utilise the SSIM score.
4. You can store a certain amount of secret info in an image, and that's called its capacity.
5. The stego image's resilience is its resistance to steganalysis attacks.

III. I. *INCEPTION V2*

One module that attempted to simplify convolution networks was Inception V2. With this module, the convolution network will be wider instead of deeper. Inception V2's three module kinds are A, B, and C. In figure 3, they are shown. Figure 3.a shows that the first module (A) switched out the 5x5 convolution for a 3x3 one. Spatial aggregation across lower-dimensional embedding may be achieved with little to no loss of representational strength, according to this approach. The 3x3 convolution improved convolution performance [8]. After dividing n x n convolutions into 1 x n and n x 1 convolutions, they found that their method was 33% cheaper than the single 3x3 convolution [8]. Module B was shown in Figure 3.b. Another improvement was an expansion of the filter based on the idea that higher-dimensional representations are simpler to handle at the network node level. Figure 3.c [31] showed the enlarged module.

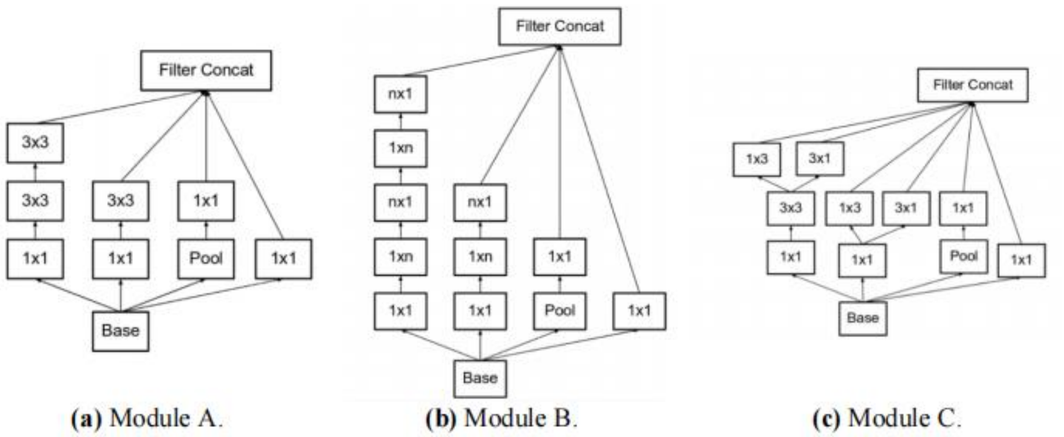

Fig 1. Module Inception V2

III.II *OPTIMISATION OF ARTIFICIAL BEE COLONIES*

In 2005 [32], Karaboga introduced the ABC algorithm. This optimisation is an optimisation strategy for numerical problems based on swarm-based meta-heuristics. The ingenuity of honey bees' foraging habits inspired its development. The algorithm is based on the one that Tereshko and Loengarov (2005) created for the foraging behaviour of honey bee colonies. Foragers with jobs, foragers without jobs, and food sources are the three main parts of the model. Part three of the system is the hive, and parts one and two, the working and unemployed foraging bees, look for food sources close by. In addition to defining self-organization and collective intelligence, the notion also defines two important behavioral patterns. In the case of abundant food supplies, forager recruitment is leading to positive feedback, whereas in the case of deficient food sources, forager desertion is leading to negative feedback. These are the main patterns of behaviour.

In ABC (for necessary problem, excellent solutions), a colony of artificial forager bees—also called agents—seeks for abundant artificial food supply. To use the ABC technique, first change the optimization scenario in question into the issue of discovering the parameter vector that most effectively minimizing an objective function. The artificial bees will first acquire of initial solution vectors a population at random, and then they will iteratively enhance them by using the strategies: migrating onto effective alternatives using a neighbor search mechanism, whilst discarding inferior answers.

III.III *AN ANALYSIS OF WAVELETS*

The wavelet transform can be used to translate a spatial domain into a frequency domain. The foundation for using wavelets in image stenographic models is the fact that, pixel-by-pixel, the wavelet transform clearly separates the high frequency information from the low frequency information. Deterministic Wavelet Transforms (DWT) are preferred over Deterministic Cosine Transforms (DCT) since low-frequency pictures at different levels can provide the required resolution. The DWT is a discrete wavelet transform with one dimension. an application of the repeating filter bank technique, processes the input after a high-pass and low-pass filter convolve it. The outcome of the second convolution is a smoother version of the input, while the first convolution is responsible for capturing the high frequency element of the signal. As part of the rebuilding procedure, the synthesis filter is used to conduct convolution, and the resulting data is combined with the original data.The one-dimensional transform is applied to all rows in a single phase in preparation for the two-dimensional transform requires that you first repeat this process for all columns. The four groups, or band coefficients, that result from this decomposition are as follows.

When it comes to wavelet transformations, the simplest one is the Haar Wavelet Transform. By averaging the two pixels' values, we can get the low frequency wavelet coefficient in this example. To get the high frequency wavelet coefficient, we divide the difference in value between two identical pixels in half. A total of four bands were identified by the findings: the horizontal (HL), vertical (LH), approximation (LL), and diagonal detail (HH) bands. The approximation band, made up of low-frequency wavelet coefficients, holds a significant portion of the spatial domain picture. Often called the detail bands, the other bands consist of high frequency coefficients. Details regarding the spatial domain image's edges are conveyed by these bands. [33].

IV. RESULTS AND DISCUSSION

IV.I *DATASET 1*

IV.I.I *DATASET USED*

A number of methods may be explored using the built-in dataset to analyse the information from computed tomography scans linked to contrast use and patient age. Identifying statistical patterns, picture

textures, and attributes that correlate highly with these traits is the main goal of this research. Furthermore, basic methods for automatically reclassifying misclassified photos (or identifying outliers, such as suspicious instances, erroneous measurements, or improperly calibrated devices) are within reach. These numbers represent a tiny fraction of the total number of photographs held by the cancer imaging database. These are the results of analysing the centre slice of all the CT scans for valid age, modality, and contrast tags. As a result, there are 475 series derived from 69 distinct patients. Sample Dataset Images are given in fig 2. Number of TIFF images is 100. Shape of the dataset is (100, 128, 128).
https://www.kaggle.com/datasets/kmader/siim-medical-images?select=tiff_images

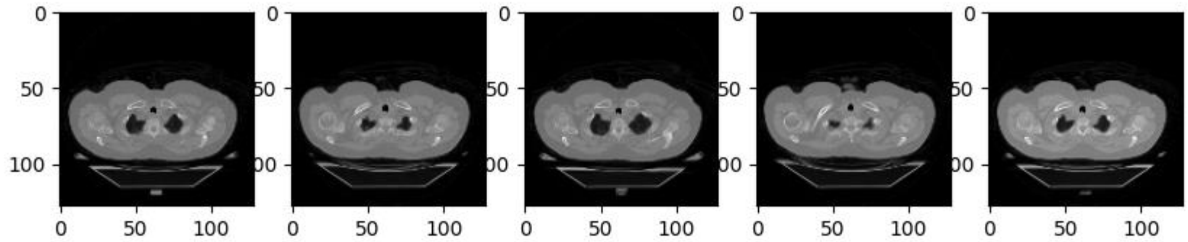

Fig 2 : Sample Dataset Images

IV.II *PREPROCESSING STEPS*

Every image in the collection goes through a series of pre-processing procedures. Normalising images and image denoising are the two pre-processing steps ued in the proposed research. An often-used technique in image processing, picture normalisation adjusts the brightness and contrast range of individual pixels to create a more visually appealing final product. "Normalisation" is altering an input image so that its pixel values are more visually typical. This is how the tool is designed to work. Fig. 3 gives the image after normalization.

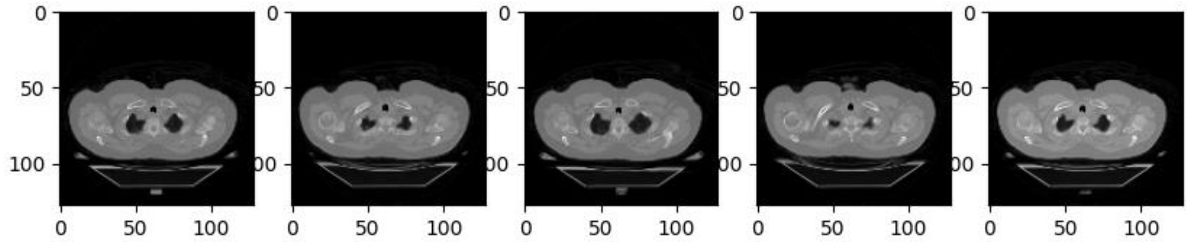

Fig. 3: Normalization

Restoring a genuine image from a noisy one is the goal of image denoising. Denoising a picture, however, might make it impossible to tell noise, edges, and textures apart since they are all high-frequency things. Hence, it's probable that the denoised images would lose some details. A major difficulty in modern times is recovering relevant information from noisy images while reducing noise to produce high-quality photographs. Denoising of images is given in fig, 4.

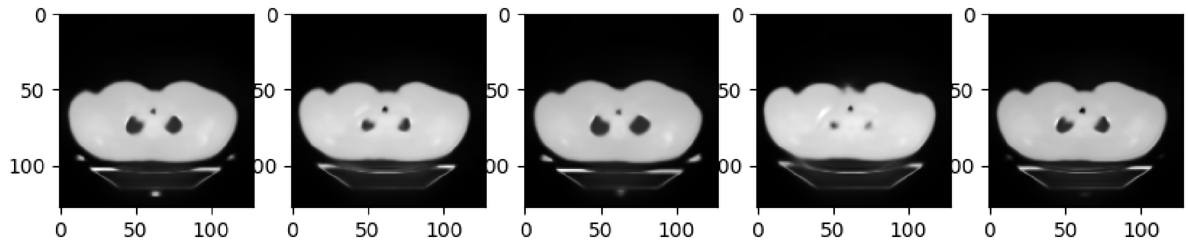

Fig.4: Denoising of images

IV.I.II *WAVELET TRANSFORM*

Wavelet transform is used for dimensional reduction in the proposed research. By eliminating redundant information and maintaining the image's original characteristics, the wavelet transform is also used to reduce the dimensionality of images. Transform Dimension is (100, 8). After dimension reduction, fetching Overview Data File is given in fig 5.

	Age	Contrast	ContrastTag	raw_input_path	id	tiff_name	dicom_name
0	60	True	NONE	../data/50_50_dicom_cases\Contrast\00001 (1).dcm	0	ID_0000_AGE_0060_CONTRAST_1_CT.tif	ID_0000_AGE_0060_CONTRAST_1_CT.dcm
1	69	True	NONE	../data/50_50_dicom_cases\Contrast\00001 (10).dcm	1	ID_0001_AGE_0069_CONTRAST_1_CT.tif	ID_0001_AGE_0069_CONTRAST_1_CT.dcm
2	74	True	APPLIED	../data/50_50_dicom_cases\Contrast\00001 (11).dcm	2	ID_0002_AGE_0074_CONTRAST_1_CT.tif	ID_0002_AGE_0074_CONTRAST_1_CT.dcm
3	75	True	NONE	../data/50_50_dicom_cases\Contrast\00001 (12).dcm	3	ID_0003_AGE_0075_CONTRAST_1_CT.tif	ID_0003_AGE_0075_CONTRAST_1_CT.dcm
4	56	True	NONE	../data/50_50_dicom_cases\Contrast\00001 (13).dcm	4	ID_0004_AGE_0056_CONTRAST_1_CT.tif	ID_0004_AGE_0056_CONTRAST_1_CT.dcm
5	48	True	NONE	../data/50_50_dicom_cases\Contrast\00001 (14).dcm	5	ID_0005_AGE_0048_CONTRAST_1_CT.tif	ID_0005_AGE_0048_CONTRAST_1_CT.dcm

Fig. 5: Fetching Overview Data File

The overview Data File is analysedon the basis of the contrast tag as given in fig. 6, on the basis of the age frequency as represented in fig. 7 and on the basis of the DICOM frequency as given in fig. 8.

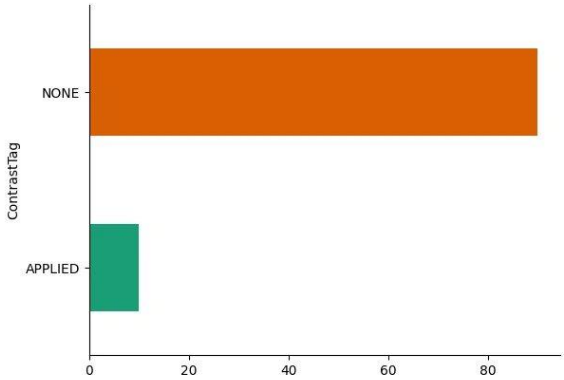

Fig. 6: Label Count

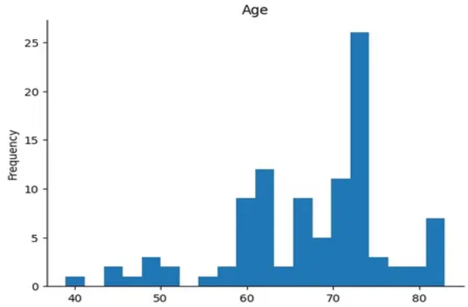

Fig 7: Age Frequency

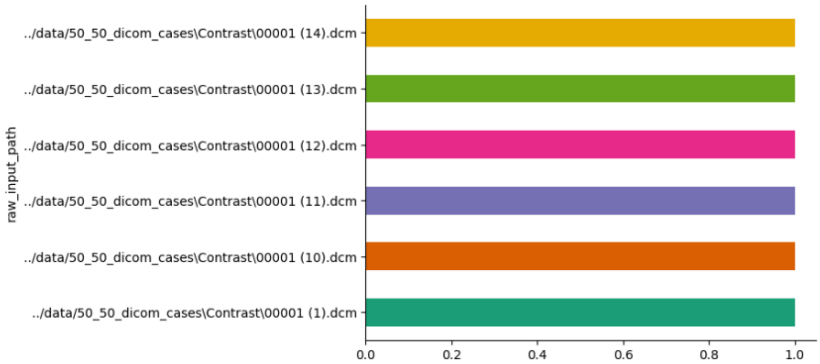

Fig. 8: DICOM Frequency

Since we are working on image steganography, a text is hidden in between the images. In the proposed research, randomly generated texts are created and the Text Transformer is used for the text to number conversion. These numerical data will be added to the images as image steganography.

```
0110100001100101011011000110110001101111
hello
```

Next, ((75, 128, 128), (25, 128, 128)), (75, 2), (25, 2)) is the dataset divided proportionally between training and testing, with 75% of the total. Its form is (128, 128) for the single picture.

IV. I. III *INCEPTION V2 BASED AUTOENCODER*

Configuration of Inception V2 based Autoencoder is completed. Configuring ABC Optimizer and executing ABC. When attempting to solve a problem that does not have a local optimum solution, you may either look for the global optimal solution or attempt to solve the problem using a local optimal solution. Finding the best answer to a problem might be a part of global optimization, which entails analysing multiple local optimal solutions. The global objective graph and the local objective graph is given in fig. 9. At the local level [in 1 cluster] and at the global level (in all data), this graph shows the trajectory, each epoch, of the time required to identify an optimal point (X).

Fig 10 displays both the global and local fitness graphs. Fig. 11 shows the runtime chart, which shows how long it takes to process the dataset. Exploration refers to any activity that gives the agent the opportunity to learn about new aspects of the environment, whereas exploitation refers to making use of knowledge that has already been acquired. If the agent continues to rely solely on its previous experiences, it will almost certainly become mired in a policy that is less than ideal.

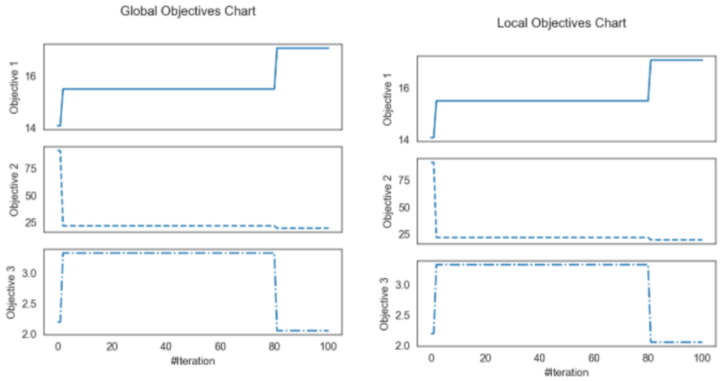

Fig. 9: Global and Local Objectives chart

Global and Local Best Fitness

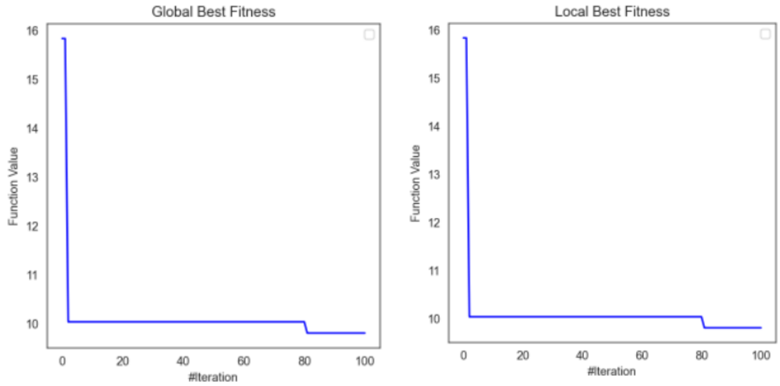

Fig10: Global and Local Best Fitness

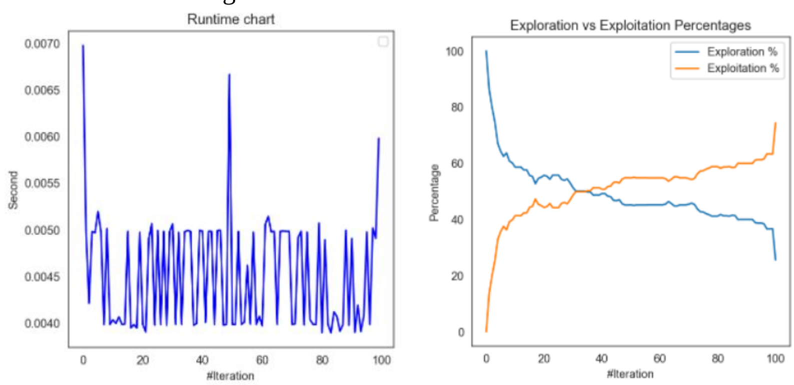

Fig.11: Runtime and Exploration/Exploitation Chart

ABC's Best Optimum Points is [20, 8]. This optimum point is used for training of the images using Inception V2 based autoencoder. Encoded Image is created by inserting the random text into the image using Encoder. Fig. 12 shows the representation of the encoded images after text insertion in images.

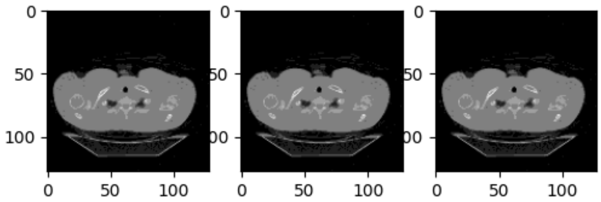

Fig. 2: Encoded Images

Reshaped Data and Encoded Image for Training is ((75, 128, 128, 1) (Reshaped or original image), (75, 128, 128, 1) (Encoded image with the text), (25, 128, 128, 1)) Testing set of the reshaped image).

Model Accuracy to Loss Graph is given in figure 4.9. Model Accuracy to Loss Ratio is given in fig. 13. The number of accurate predictions obtained is called the accuracy score. When compared to the intended goal state (or states), loss numbers show how far off the mark we are.

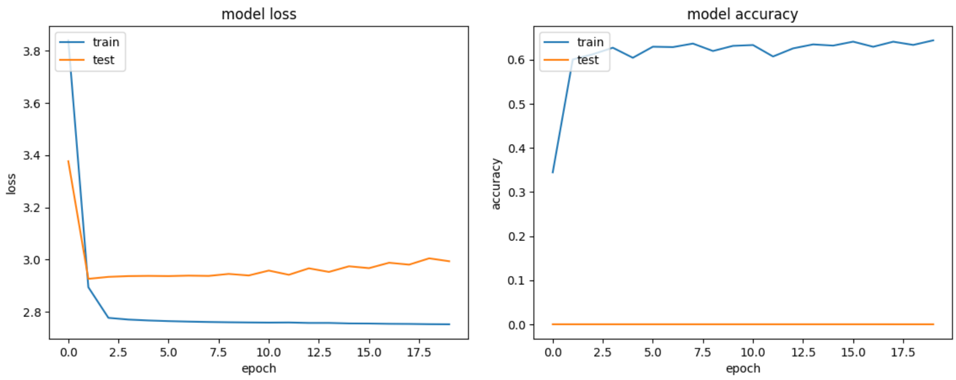

Fig. 13: Model Accuracy to Loss Graph

After testing and prediction, the decoded Images Shape is (25, 128, 128, 1). Prediction and Scores are
Original Text in Image: - 5M5XUlp9A3
Predicted Text in Image: - 5M5XUlp9A3
After testing and Prediction for all data, the text extraction accuracy is 91.00%.

DWT Coefficients are used for analysing the dataset. The DWT coefficients provide temporal information about the studied signal since they show the strength of correlation between the wavelet function and the examined signal at various points in time. DWT Coefficients Calculation is used to calculate the robustness. It is the correlation matrx based on the dwt techniques.

```
        [ 0. ,  0. ,  0. , ...,  0. ,  0. ,  0. ],
        [ 0. ,  0. ,  0. , ...,  0. ,  0. ,  0. ]])),
(array([[0. , 1. , 0.5, ..., 1. , 1. , 0.5],
        [0. , 0. , 0. , ..., 0. , 0. , 0. ],
        [0. , 0. , 0. , ..., 0. , 0. , 0. ],
        ...,
        [0. , 0. , 0. , ..., 0. , 0. , 0. ],
        [0. , 0. , 0. , ..., 0. , 0. , 0. ],
        [0. , 0. , 0. , ..., 0. , 0. , 0. ]]),
 array([[0. , 1. , 0.5, ..., 1. , 1. , 0.5],
        [0. , 0. , 0. , ..., 0. , 0. , 0. ],
        [0. , 0. , 0. , ..., 0. , 0. , 0. ],
        ...,
        [0. , 0. , 0. , ..., 0. , 0. , 0. ],
        [0. , 0. , 0. , ..., 0. , 0. , 0. ],
        [0. , 0. , 0. , ..., 0. , 0. , 0. ]]),
 array([[ 0. ,  0. , -0.5, ...,  0. ,  0. ,  0.5],
        [ 0. ,  0. ,  0. , ...,  0. ,  0. ,  0. ],
        [ 0. ,  0. ,  0. , ...,  0. ,  0. ,  0. ],
        ...,
        [ 0. ,  0. ,  0. , ...,  0. ,  0. ,  0. ],
        [ 0. ,  0. ,  0. , ...,  0. ,  0. ,  0. ],
        [ 0. ,  0. ,  0. , ...,  0. ,  0. ,  0. ]]),
 array([[ 0. ,  0. , -0.5, ...,  0. ,  0. ,  0.5],
        [ 0. ,  0. ,  0. , ...,  0. ,  0. ,  0. ],
        [ 0. ,  0. ,  0. , ...,  0. ,  0. ,  0. ],
        ...,
        [ 0. ,  0. ,  0. , ...,  0. ,  0. ,  0. ],
```

PSNR Calculation for Some Images are

```
[81.11929233160711, 66.74699841562989, 70.05402974167372, 81.11929233160711]
```

SSIM Calculation for Some Images are

```
/usr/local/lib/python3.10/dist-packages/skimage/_shared/utils.py:348: UserWarning: Inputs have mismatched dtype.  Setting data_range based on im1.dtype.
  return func(*args, **kwargs)
[0.8441091468870954,
 0.3169666539672222,
 0.47465406836870194,
 0.8441091468870954]
```

Capacity Calculation (Assuming each bit of each pixel can carry one bit of information) is 65536
Robustness Calculation (Example metric, you may want to implement a more sophisticated steganalysis approach) is
0.601068512110727 Overall Scores are
Text Extraction Accuracy: 91.00%
PSNR Score Mean: 74.75990320512946
SSIM Score Mean: 0.6199597540275288
Capacity: 65536 bits
Robustness: 0.601068512110727 err

The proposed technique, Inception V2 based Autoencoder is ompared with CNN Based Autoencoder Model. The model is trained and the Model Loss Graph is considered as represented in fig 12.

Fig. 12: Model Loss Graph

After testing and Evaluation, the decoded Image Shape is (25, 128, 128, 1). After reshaping back to the original images, the model Accuracy is

```
 Text Extraction Accuracy: 55.11%
```

DWT Coefficients Calculation

```
          [-1.5826139e-05, -7.3166928e-05,  9.6242322e-05, ...,
           -2.0715175e-05, -9.4345720e-05,  1.2966478e-04],
          [ 6.3852480e-05,  1.2814748e-04, -5.5338824e-05, ...,
            7.1228278e-06, -1.9503455e-04,  7.0385235e-05],
          [ 4.2682112e-04,  3.6857411e-05, -1.2228909e-04, ...,
           -1.2799999e-04,  4.5086589e-04, -4.3729460e-04]], dtype=float32)),
  (array([[0.9993377 , 0.99856293, 0.99892354, ..., 0.9983753 , 0.9982608 ,
           0.9997298 ],
          [0.9989538 , 0.9974438 , 0.998242  , ..., 0.99849033, 0.9978465 ,
           1.000376  ],
          [0.9983698 , 0.9969728 , 0.99796474, ..., 0.9983467 , 0.9980873 ,
           1.0011749 ],
          ...,
          [0.9981961 , 0.99693006, 0.99787664, ..., 0.99807036, 0.9978787 ,
           1.001065  ]
```

PSNR Calculation for Some Images

```
[47.30919789657161, 47.309704676308]
```

SSIM Calculation for Some Images

```
/usr/local/lib/python3.10/dist-packages/skimage/_shared/utils.py:348: UserWarning: Inputs have mismatched dtype.  Setting data_range based on im1.dtype.
  return func(*args, **kwargs)
[0.3127541734370671, 0.2936828871542703]
```

Capacity Calculation (Assuming each bit of each pixel can carry one bit of information): 32768
Robustness Calculation (Example metric, you may want to implement a more sophisticated steganalysis approach)
0.60059269240841695
Overall Scores

Text Extraction Accuracy: 55.11%
PSNR Score: 47.30945128643981
SSIM Score: 0.3032185302956687
Capacity: 32768 bits
Robustness: 0.60059269240841695 err

IV. II *DATASET 2*

The brain MRI Image Dataset is used for analyzing the proposed method. As per IBM, computer vision models are engineered to extract significant data from digital photos and movies. It makes considerable use of medical picture data to improve disease prediction, diagnosis, and treatment. The original image is given in figure 4.14. The shape of the image is (100, 128, 128).

Link: - https://www.kaggle.com/datasets/navoneel/brain-mri-images-for-brain-tumor-detection

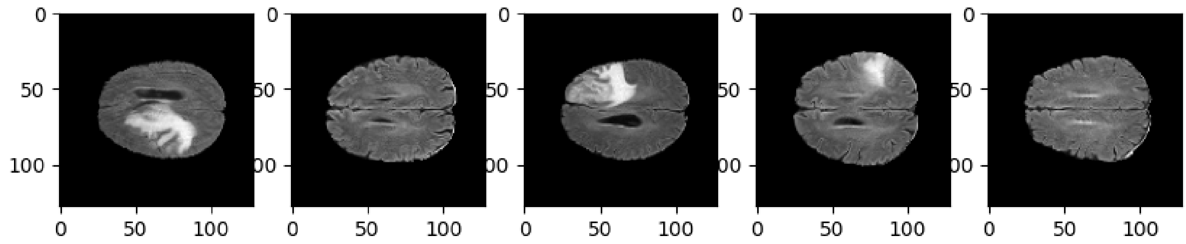

Fig. 13 : Original Image

The preprocessing steps applied are normalization and denoising. The normalized image are represented in fig. 14 and the denoised images are represented in fig.15.

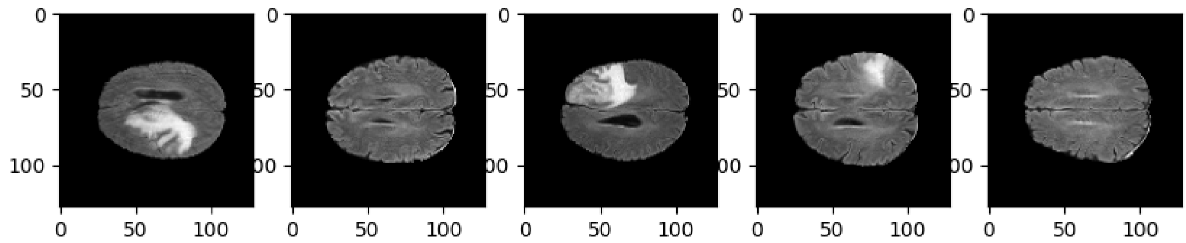

Fig.14: Normalized Image

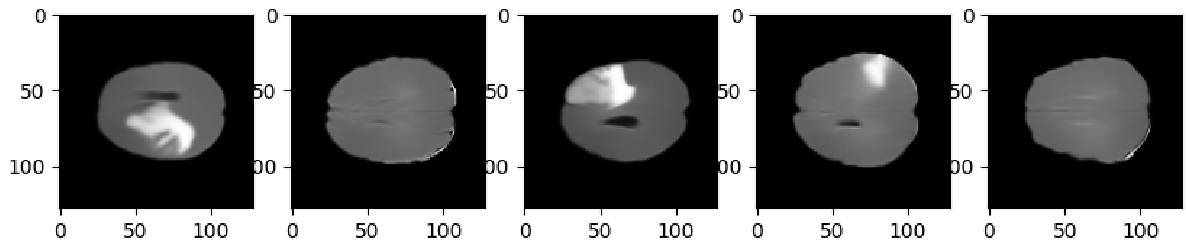

Fig. 15: Denoised Image

The wavelet Transform used is given as follows

```
<ipython-input-15-ae46f8f5e977>:5: VisibleDeprecationWarning: Creating an ndarray from ragged nested sequences (which is a list-or-tuple of lists-or-tuples-or ndarrays with different l
  wavelet_transformed_images.append(np.array(wavelet_coeffs))
```

And the wavelet Dimension is (100. 8). After fetching Overview Data File,

	Brats20ID	Age	Survival_days	Extent_of_Resection
0	BraTS20_Training_001	60	289	GTR
1	BraTS20_Training_002	52	616	GTR
2	BraTS20_Training_003	54	464	GTR
3	BraTS20_Training_004	39	788	GTR
4	BraTS20_Training_005	68	465	GTR

Overview Data File Analysis is completed.

The label Count is given in fig.16, the age frequency is given in fig. 17 and the survival frequency is given in fig. 18.

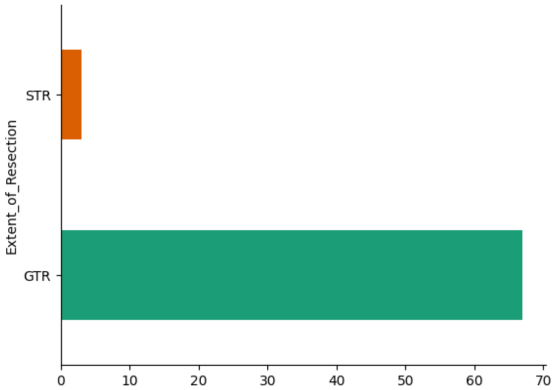

Fig.16: Label count

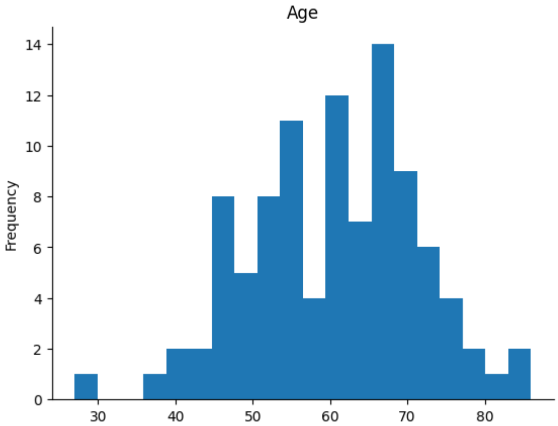

Fig. 17: Age Frequency

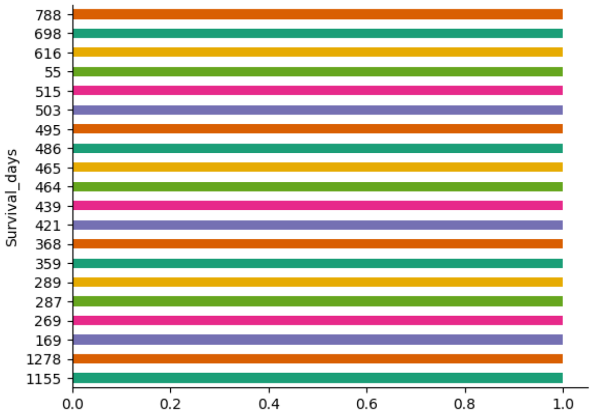

Fig. 18: Survival Frequency

After applying the label Encoder, the text Transformer is applied and then the dataset is split into Train Test dataset in the ratio, (75-25%). The dimensions of the split dataset is ((75, 128, 128), (25, 128, 128)), (75, 2), (25, 2). The single Image Shape is (128, 128).

Configuration Inception V2 based Autoencoder and configuring ABC Optimizer, the ABC Execution takes place. The ABC's Best Optimum Points obtained are [10, 8]. Next, encoded Image is created with hidden text using Encoder and the encoded Images are given in fig.19.

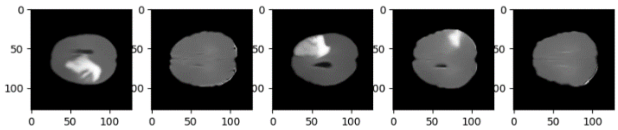

Fig. 19: Encoded images

Reshaping Data and Encoded Image for Training, ((75, 128, 128, 1), (75, 128, 128, 1), (25, 128, 128, 1))
After training Inception V2 Autoencoder Model, the model Accuracy to Loss Graph obtained is given in fig. 20.

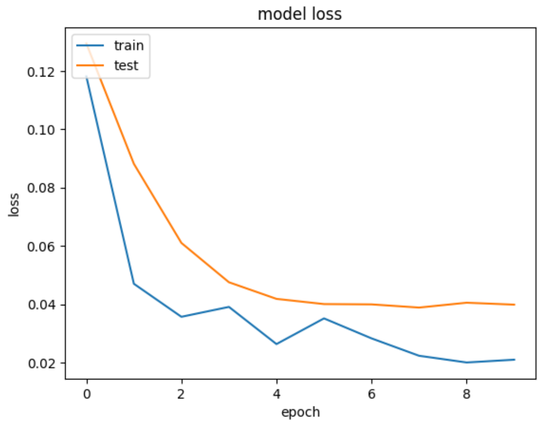

Fig. 20: Model Accuracy to Loss Graph

After testing And Evaluation, the decoded Images Shape is (25, 128, 128, 1).
The prediction and Scores are
Original Text in Image: - fkiuPDaeCl
Predicted Text in Image: - fkiuPDaeCl
Testing and Prediction for all data, the accuracy obtained is

```
Text Extraction Accuracy: 74.67%
```

The DWT Coefficients Calculation is as given,

```
(array([[0.5, 0.5, 0.5, ..., 1. , 1. , 0.5],
        [0. , 0. , 0. , ..., 0. , 0. , 0. ],
        [0. , 0. , 0. , ..., 0. , 0. , 0. ],
        ...,
        [0. , 0. , 0. , ..., 0. , 0. , 0. ],
        [0. , 0. , 0. , ..., 0. , 0. , 0. ],
        [0. , 0. , 0. , ..., 0. , 0. , 0. ]]),
 array([[0.5, 0.5, 0.5, ..., 1. , 1. , 0.5],
        [0. , 0. , 0. , ..., 0. , 0. , 0. ],
        [0. , 0. , 0. , ..., 0. , 0. , 0. ],
        ...,
        [0. , 0. , 0. , ..., 0. , 0. , 0. ],
        [0. , 0. , 0. , ..., 0. , 0. , 0. ],
        [0. , 0. , 0. , ..., 0. , 0. , 0. ]]),
 array([[-0.5,  0.5, -0.5, ...,  0. ,  0. ,  0.5],
        [ 0. ,  0. ,  0. , ...,  0. ,  0. ,  0. ],
        [ 0. ,  0. ,  0. , ...,  0. ,  0. ,  0. ],
        ...,
        [ 0. ,  0. ,  0. , ...,  0. ,  0. ,  0. ],
        [ 0. ,  0. ,  0. , ...,  0. ,  0. ,  0. ],
        [ 0. ,  0. ,  0. , ...,  0. ,  0. ,  0. ]]),
 array([[-0.5,  0.5, -0.5, ...,  0. ,  0. ,  0.5],
        [ 0. ,  0. ,  0. , ...,  0. ,  0. ,  0. ],
        [ 0. ,  0. ,  0. , ...,  0. ,  0. ,  0. ],
        ...,
        [ 0. ,  0. ,  0. , ...,  0. ,  0. ,  0. ],
        [ 0. ,  0. ,  0. , ...,  0. ,  0. ,  0. ],
        [ 0. ,  0. ,  0. , ...,  0. ,  0. ,  0. ]])),
```

PSNR Calculation for Some Images

```
68.13483767749989,
67.7393797695828,
67.7924954619976,
67.13258777582696,
70.95467354263815,
67.52022877737055,
69.79295052820493,
67.55611456846918,
66.3624466725613,
67.5027942639368,
66.4701990484174,
65.87081853426476,
69.54542228259966,
69.51821050557915,
65.17180588677793,
68.72425289072721,
66.60338184520867,
70.29366958077554,
67.74423540060845,
68.74257193393908,
```

SSIM Calculation for Some Images

```
[0.6533443912048577,
 0.6248769665652809,
 0.6526147545664288,
 0.627595832060987,
 0.6175457542063193,
 0.6400906718442902,
 0.6208257810474235,
 0.6410798853177063,
 0.6125018102147877,
 0.6302433206406087,
 0.6154930069185441,
 0.6355752506673767,
 0.6099711721190566,
 0.6065049826923009,
```

Capacity Calculation (Assuming each bit of each pixel can carry one bit of information)
1228800
Robustness Calculation (Example metric, you may want to implement a more sophisticated steganalysis approach)
0.21005964175690475
Overall Scores
Text Extraction Accuracy: 74.67%
PSNR Score: 68.11767634141208
SSIM Score: 0.600746824139316
Capacity: 1228800 bits
Robustness: 0.21005964175690475 err

The proposed method is compared with the CNN Based Autoencoder Model
After model training the model Loss Graph is given in fig. 21.

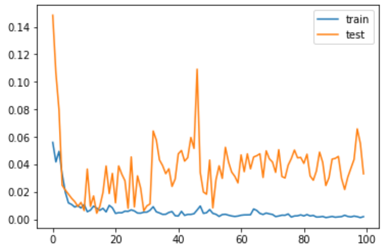

Fig. 21: Model Loss Graph

After testing and Evaluation, decoded Image Shape is (25, 128, 128, 1). After reshaping, the Model Accuracy obtained is
Text Extraction Accuracy: 52.86%
Overall Scores
Text Extraction Accuracy: 52.86%
PSNR Score: 49.862515265
SSIM Score: 0.380145256201
Capacity: 32685 bits
Robustness: 0.485256552 err

IV.III *DATASET* 3

You can compare it to the original dataset using the chest X-Ray Images (Pneumonia) Dataset. Each image category (Pneumonia/Normal, for example) has its own subfolder within the larger "train," "test," and "val" folders in the dataset. There are 5,863 JPEG X-ray photographs divided into two groups: normal and pneumonia.

From retrospective cohorts, we chose chest X-rays of children aged one to five taken at the Guangzhou Women and Children's Medical Centre in Guangzhou. Every time, we X-rayed the patient's chest as part of their regular care.

All radiographs were reviewed for quality control before chest x-ray photo analysis. Low-quality or unreadable scans were removed. Two doctors who are board-certified in medicine reviewed the images before the AI system was trained on them. We double-checked the assessment set to exclude the possibility of grading errors. Fig. 22 displays the Original Image. The dataset has the form (100, 128, 128).
Link: - https://www.kaggle.com/datasets/paultimothymooney/chest-xray-pneumonia

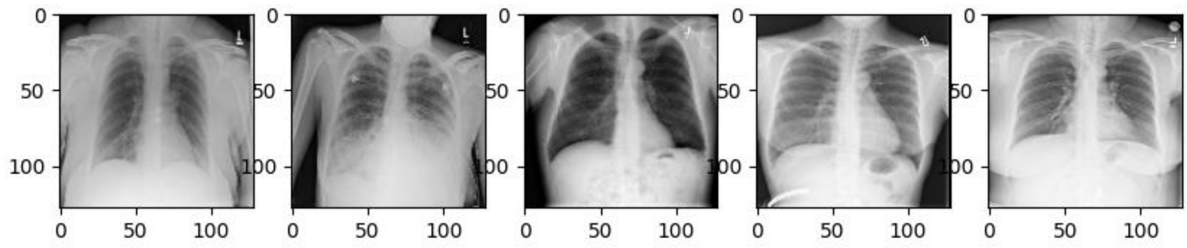

Fig. 22 : Original Image

After preprocessing the Normalized Image is given in fig. 23, the Denoised Image is given in fig. 24.

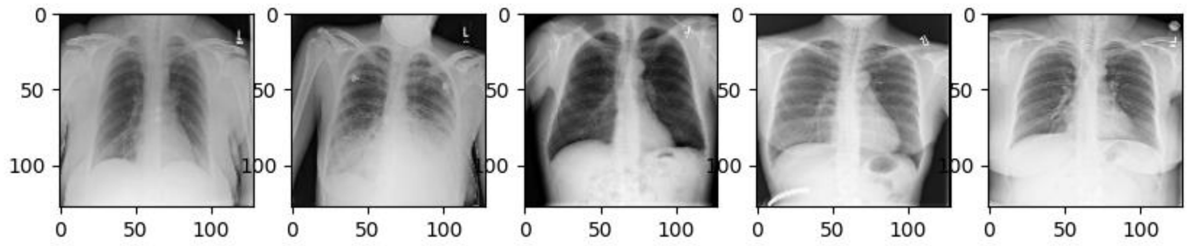

Fig. 23: Normalized Image

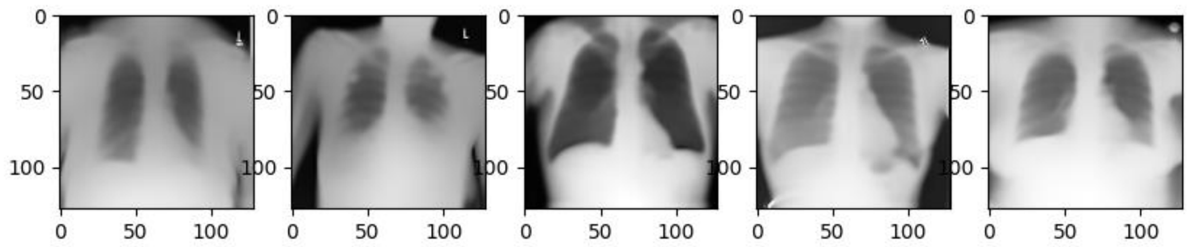

Fig. 24: Denoised Image

The wavelet Transform is used for dimension reduction,

```
<ipython-input-15-ae46f8f5e977>:5: VisibleDeprecationWarning: Creating an ndarray from ragged nested sequences (which is a list-or-tuple of lists-or-tuples-or ndarrays with different l
  wavelet_transformed_images.append(np.array(wavelet_coeffs))
```

And the wavelet Dimensions are (100, 8). The text Transformer used is

```
01110111011011110111001001101011
work
```

The dataset is split into train and Test dataset in the ratio, (75-25%)
((75, 128, 128), (25, 128, 128)), (75, 2), (25, 2)
Single Image Shape is (128, 128). Configuration Inception V2 based Autoencoder and configuring ABC Optimizer, ABC is Executed. The ABC's Best Optimum Points are [10, 8]. Create Encoded Image with hidden text using Encoder and the encoded Images are represented in fig. 25.

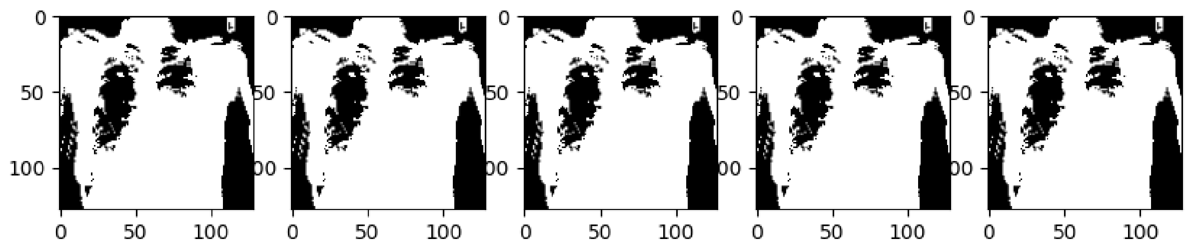

Fig. 25: encoded Images

Reshaping Data and Encoded Image for Training in the ratio,
((75, 128, 128, 1), (75, 128, 128, 1), (25, 128, 128, 1))
Training Inception V2 Autoencoder Model, the Model Accuracy to Loss Graph obtained is given in fig. 26.

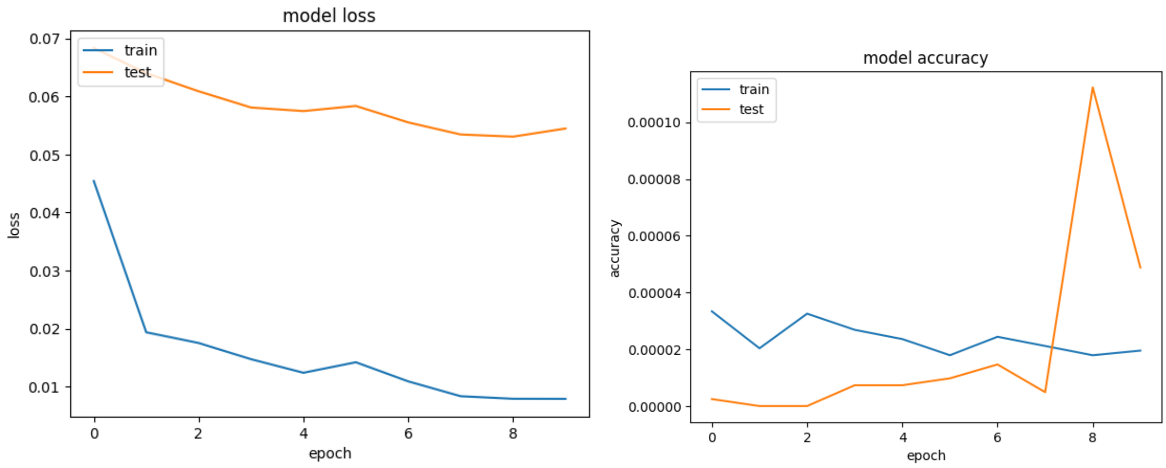

Fig. 26: Model Accuracy to Loss Graph

After testing And Evaluation, the decoded Images Shape
(25, 128, 128, 128)
Prediction and Scores
Original Text in Image: - u1q6PM764Z
Predicted Text in Image: - u1q6PM764Z
After testing and Prediction for all data

```
p_text = []
for i in range(len(x_train)):
    original_img = x_train[i].reshape((128, 128)).astype(np.uint8)
    result = str(decode(encoded_images[i]))
    #print(result)
    p_text.append(result)
```

Accuracy:

```
Text Extraction Accuracy: 73.33%
```

Overall Scores
Text Extraction Accuracy: 73.33%
PSNR Score: 62.2239261908548
SSIM Score: 0.36131035862715977
Capacity: 1228800 bits
Robustness: 0.8736081880000004 err

The proposed Inception V2 based autoencoder is compared with the CNN Based Autoencoder Model. After model training the Model Loss Graph obtained is given in fig. 27.

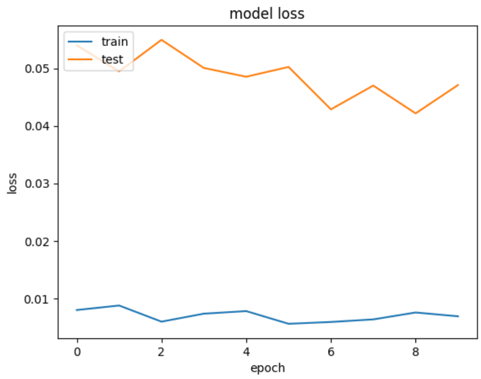

Fig. 27: Model Loss Graph

After testing and Evaluation, the decoded Image Shape is (25, 128, 128, 1). After reshaping, the ,odel Accuracy obtained is

Text Extraction Accuracy: 22.42%

Overall Scores
Text Extraction Accuracy: 22.42%
PSNR Score: 66.29536458801716
SSIM Score: 0.5982152471046789
Capacity: 409600 bits
Robustness: 2.7436830373549252 err

V. CONCLUSION

This project proposes a new image steganography technique that uses Inception V2 and wavelet transform with hyperparameter tuning through ABC which make it an Ensemble Inception V2 Model. The difficulty in detecting the existence of secret data in the stego image suggests that this technique could be more secure than typical image steganography methods. The project will also compare the performance of the Inception V2 based autoencoder model with CNN based autoencoder model. Three datasets are used for comparison and the first dataset is having an accuracy for the proposed Inception V2 based autoencoder model of 91.00%.

REFERENCES

[1]. S. Kaur, S. Singh, M. Kaur, and H.-N. Lee, *A Systematic Review of Computational Image Steganography Approaches* Archives of Computational Methods in Engineering, vol. 29, no. 7, pp. 4775–4797, Nov.2022, https://doi.org/10.1007/s11831-022-09749-0.

[2]. M. Hussain, A. W. A. Wahab, Y. I. B. Idris, A. T. S. Ho, and K.-H.Jung, *Image steganography in spatial domain: A Survey* Signal Processing: Image Communication, vol.65, pp.46–66, Jul.2018, https://doi.org/10.1016/j.image.2018.03.012.

[3]. G. M. Naidoo, "Digital Communication: Information CommunicationTechnology (ICT) Usage for Teaching and Learning," in *Handbook of Research on Digital Learning*, Hershey, PA, USA: IGI Global, 2020, pp.1–19.

[4]. J. Prinsloo, S. Sinha, and B. von Solms, A Review of Industry 4.0 Manufacturing Process Security Risks, Applied Sciences, vol. 9, no.23, Jan.2019, Art.no. 5105, https://doi.org/10.3390/app9235105.

[5]. J. Qin, Y. Luo, X. Xiang, Y. Tan, and H. Huang, *Coverless Image Steganography: A Survey*, IEEE Access, vol. 7, pp. 171372–171394, 2019, https://doi.org/10.1109/ACCESS.2019.2955452.

[6]. A. Baksi, S. Bhasin, J. Breier, D. Jap, and D. Saha, *A Survey on FaultAttacks on Symmetric Key Cryptosystems*, ACM Computing Surveys, vol. 55, no.4, Aug.2022, Art.no.86, https://doi.org/10.1145/3530054.

[7]. J.Herranz, *Attacking Pairing – Free Attribute – Based Encryption Schemes*, IEEE Access, vol.8, pp.226 – 232, 2020, https://doi.org/10.1109/ACCESS.2020.3044143.

[8]. R. Din, M. Mahmuddin, and A. J. Qasim, *Review on steganographymethods in multi-media domain*, International Journal of Engineering & Technology, vol.8, no.1.7, pp.288–292, 2019.

[9]. Y. Xu, C. Mou, Y. Hu, J. Xie, and J. Zhang, *Robust Invertible Image Steganography*, in IEEE / CVF Conference on Computer Vision and Pattern Recognition, New Orleans, LA, USA, Jun. 2022, pp. 7865–7874, https://doi.org/10.1109/CVPR52688.2022.00772.

[10]. Z. Wang, G. Feng, Z. Qian, and X. Zhang, *JPEG Steganography WithContent Similarity Evaluation*, IEEE Transactions on Cybernetics, pp.1–12, 2022,https://doi.org/10.1109/TCYB.2022.3155732.

[11]. D.R.I.M.Setiadi, *Improved payload capacity in LSB Image Steganography uses dilated hybrid edge detection*, Journal of King Saud University – Computer and Information Sciences, vol.34, no.2, pp.104–114, Oct.2022, https://doi.org/10.1016/j.jksuci.2019.12.007.

[12]. M. Kumar, A. Soni, A. R. S. Shekhawat, and A. Rawat, *EnhancedDigital Image and Text Data Security Using Hybrid Model of LSB Steganography and AES Cryptography Technique*, in Second International Conference on Artificial Intelligence and Smart Energy, Coimbatore, India, Feb. 2022, pp. 1453–1457, https://doi.org/10.1109/ICAIS53314.2022.9742942.

[13]. S. Roy and Md. M. Islam, *A Hybrid Secured Approach CombiningLSB Steganography and AES Using Mosaic Images for Ensuring Data Security*, SN Computer Science, vol. 3, no. 2, Feb. 2022, Art. no. 153, https://doi.org/10.1007/s42979-022-01046-8.

[14]. S. Ghosal, S. Roy, and R. Basak, *LSB Steganography Using Three Level Arnold Scrambling and Pseudo-random Generator*, in International Conference on Network Security and Blockchain Technology, Kolkata, India, Dec. 2021, pp. 105–116, https://doi.org/10.1007/978-981-19-3182-6_9.

[15]. M.E.Saleh,A.A.Aly,andF.A.Omara, *Data Security Using Cryptography and Steganography Techniques*, International Journal of Advanced Computer Science and Applications, vol. 7, no. 6, pp. 390–397,2016, https://doi.org/10.14569/IJACSA.2016.070651.

[16]. S. Baluja, *Hiding Images in Plain Sight: Deep Steganography*, in 31stConference on Neural Information Processing Systems, Long Beach,CA,USA,Dec.2017,pp.1–11.

[17]. R.Meng, Z.Zhou, Q.Cui,X.Sun, and C.Yuan, *A Novel Steganography Scheme Combining Coverless Information Hiding and Steganography*, Journal of Information Hiding and Privacy Protection Preview publication details, vol.1, no.1, pp.43–48, 2019, https://doi.org/10.32604/jihpp.2019.05797.

[18]. S. Malalla and F.R.Shareef, *Improving Hiding Security of Arabic Text Steganography by Hybrid AES Cryptography and Text Steganography*," Journal of Engineering Research and Application, vol. 6, no. 6, pp. 60–69,Jun.2016.

[19]. M. Douglas, K. Bailey, M. Leeney, and K. Curran, *An overview ofsteganography techniques applied to the protection of biometric data*, Multimedia Tools and Applications, vol. 77, no. 13, pp. 17333–17373,Jul.2018,https://doi.org/10.1007/s11042-017-5308-3.

[20]. Q. Liu et al., *When Deep Learning Meets Steganography: Protecting Inference Privacy in the Dark*, in IEEE Conference on Computer Communications, London, United Kingdom, Dec. 2022, pp. 590–599, https://doi.org/10.1109/INFOCOM48880.2022.9796975.

[21]. F. Al-Shaarani and A. Gutub, *Increasing Participants Using Counting-Based Secret Sharing via Involving Matrices and Practical Steganography*, Arabian Journal for Science and Engineering, vol. 47, no.2, pp.2455–2477, Feb.2022, https://doi.org/10.1007/s13369-021-06165-7.

[22]. G.Peter, A.Sherine, Y.Teekaraman, R.Kuppusamy, and A.Radhakrishnan, *Histogram Shifting – Based Quick Response Steganography Method for Secure Communication,* Wireless Communications and Mobile Computing, vol. 2022, Mar. 2022, Art. no.e1505133, https://doi.org/10.1155/2022/1505133.

[23]. F.Li, Z.Yu, and C.Qin, *GAN-based spatial image steganography with cross feedback mechanism,* Signal Processing, vol.190, Jan.2022, Art.no.108341, https://doi.org/10.1016/j.sigpro.2021.108341.

[24]. A.K.Sahu and A.Gutub, *Improving grayscale steganography to protect personal information disclosure within hotel services*, Multimedia Tools and Applications, vol. 81, no. 21, pp. 30663–30683, Sep.2022, https://doi.org/10.1007/s11042-022-13015-7.

[25]. M. Yousefi Valandar, P. Ayubi, M. Jafari Barani, and B. Yosefnezhad Irani, *A chaotic video steganography technique for carrying different types of secret messages,*" Journal of Information Security and Applications, vol. 66, May 2022, Art.no.103160, https://doi.org/10.1016/j.jisa.2022.103160.

[26]. V.Sabeti and M.Amerehei, *Secure and Imperceptible Image Steganography in Discrete Wavelet Transform Using the XOR Logical Function and Genetic Algorithm,* ISeCure, vol. 14, no. 2, pp. 167–179, Jan.2022.

[27]. X. Liu, Z. Ma, J. Ma, J. Zhang, G. Schaefer, and H. Fang, *ImageDisentanglement Autoencoder for Steganography without Embedding,* in IEEE/CVF Conference on Computer Vision and Pattern Recognition, New Orleans, LA, USA, Jun. 2022, pp.2293–2302, https://doi.org/10.1109/CVPR52688.2022.00234.

[28]. R.Adee and H. Mouratidis, *ADynamicFour-Step Data Security Model for Data in Cloud Computing Based on Cryptography and Steganography*, Sensors, vol.22,no.3, Jan.2022,Art.no.1109, https://doi.org/10.3390/s22031109.

[29]. S. Hossain, S. Mukhopadhyay, B. Ray, S. K. Ghosal, and R. Sarkar, *A secured image steganography method based on ballot transform and genetic algorithm*, Multimedia Tools and Applications, vol. 81, no. 27, pp.38429–38458,Nov.2022, https://doi.org/10.1007/s11042-022-13158-7.

[30]. Q. F. Yao, Q. Y. Zhu, Z. Q. Bu, Q. Y. Liu, M. X. Quan, and W. T.Huang, "*DNA nanosensing systems for tunable detection of meta ions and molecular crypto-steganography*," Biosensors and Bioelectronics, vol.195, Jan. 2022, Art.no.113645, https://doi.org/10.1016/j.bios.2021.113645.

[31]. Alamsyah, D., &Fachrurrozi, M. (2019, March). *Faster R-CNN with inception v2 for fingertip detection in homogenous background image*. in Journal of Physics: Conference Series (Vol. 1196, p. 012017). IOP Publishing, Karaboga, D. (2010). Artificial bee colony algorithm. scholarpedia, 5(3), 6915.

[32]. Reddy, H. M., & Raja, K. B. (2009). *High capacity and security steganography using discrete wavelet transform,* International Journal of Computer Science and Security (IJCSS), 3(6), 462-472.